Journal of Thermal Science Vol.23, No.5 (2014) 465−471

DOI: 10.1007/s11630-014-0730-6 **Article ID: 1003-2169(2014)05-0465-07**

Experimental Study on Load Characteristics in a Floating Type Pendulum Wave Energy Converter

Tengen Murakami, Yasutaka Imai and Shuichi Nagata

Institute of Ocean Energy, Saga University, Saga, Japan

A floating type pendulum wave energy converter (FPWEC) with a rotary vane pump as the power take-off system was proposed by Watabe et al. in 1998. They showed that this device had high energy conversion efficiency. In the previous research, the authors conducted 2D wave tank tests in regular waves to evaluate the generating efficiency of FPWEC with a power take-off system composed of pulleys, belts and a generator. As a result, the influence of the electrical load on the generating efficiency was shown. Continuously, the load characteristics of FPWEC are pursued experimentally by using the servo motors to change the damping coefficient in this paper. In a later part of this paper, the motions of the model with the servo motors are compared with that of the case with the same power take-off system as the previous research. From the above experiment, it may be concluded that the maximum primary conversion efficiency is achieved as high as 98% at the optimal load.

Keywords: pendulum, wave energy converter, floating type, load characteristics, primary conversion efficiency

Introduction

A fixed type pendulum wave energy converter was proposed by Watabe et al. [1] firstly. They showed that this device had high energy conversion efficiency. However, in this device, about 70% of the construction cost is allocated for the caisson. Furthermore, it is difficult to maintain without the mechanical failure in storm condition like a typhoon. Therefore, Watabe proposed a floating type pendulum wave energy converter (FPWEC) with a rotary vane pump as the power take-off system. FPWEC can be installed in offshore region in order to reduce the construction cost. In addition, the offshore FPWEC is advantageous on the wave power in offshore region being larger than the wave power on shoreline. Watabe conducted the fundamental experiments in 2D wave tank to grasp the primary conversion efficiency of this device in regular waves.

And, the authors [2] conducted 2D tank tests to evaluate the generating efficiency of FPWEC in regular waves. In our experiments, a test model of FPWEC with a power take-off system composed of pulleys, belts and a generator was prepared. From this experiment, the effect of electrical load on generating efficiency was shown by comparison between three cases of the electric resistors as preliminary step.

Park et al. [3] examined the primary conversion efficiency of FPWEC by using the power take-off system composed of an electric motor and the measuring sensors. In this experiment, it seems that the torque of the pendulum shaft is not proportional to the rotational speed, that is, the torque control is incomplete. Nam et al. [4] carried out the numerical calculation of the 3D motions of FPWEC in regular and irregular waves due to the higher-order boundary element method. In this study, the motions of FPWEC are compared between the calculated

Received: June 2014
Tengen Murakami: Research Associate

result and the measured result. However, the primary conversion efficiency is unclear.

The purpose of our research is the development of the optimal design method of FPWEC based on the investigation of the fundamental performance. In this paper, the load characteristics of FPWEC and motions of the floating body in regular wave were examined experimentally by changing the pendulum position. In a latter part of the paper, the generating efficiency of the model with the power take-off system composed of pulleys, belts and a generator is shown.

Experimental Procedure

FPWEC test model with servo motors

Figure 1 shows the FPWEC test model. This model consists of a pendulum plate, two servo motors at both ends of a pendulum shaft, two side walls, back wall, bottom board, motion reduction plate, float, ballast and frames. The total length of the test model is 1340 mm long. The front half side with 675 mm long is a water chamber for pendulum and the rear half side with 665 mm long is a water pool to keep the body stable in waves. The draft is 216 mm. Two wave height gauges were located at 40 mm lee side from the pendulum plate and at 40 mm weather side from the back wall as shown in Fig. 2.

Wave tank

Figure 3 shows the arrangement of experimental devices in the two dimensional wave tank. This tank has 18.5 m long, 0.8 m width and 1.0 m depth. Two absorbing wave makers were installed at both ends of the tank. FPWEC test model was moored at the center of the tank by a wire. The force gauge is settled at the other end of the wire. And also, to keep the test model at the center of the tank, we pulled model to lee side by using nylon lines. The initial tension of nylon lines is 1 N. Eight wave gauges were arranged in order to measure the amplitudes of incident wave, reflected wave and transmitted wave accurately. The motions of the floating body in regular wave were measured by optical motion capture system HALCON. The incident wave height is 0.015 m.

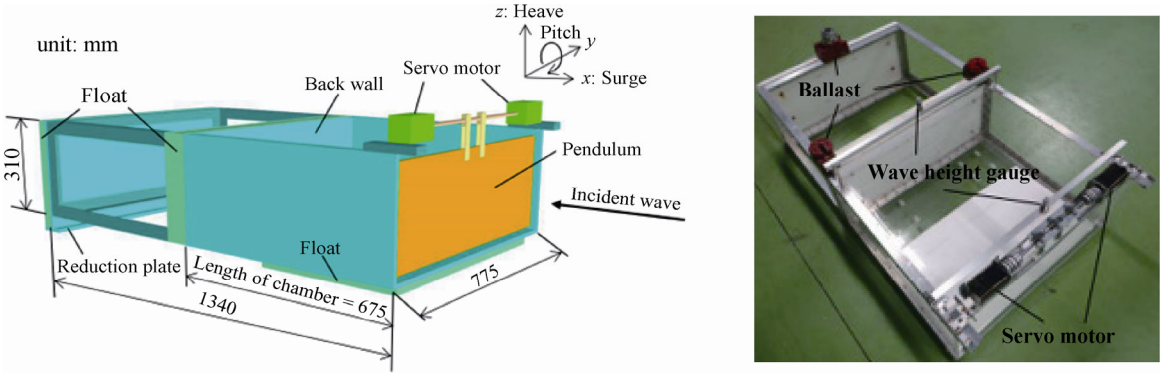

Fig. 1 Experimental model with servo motors.

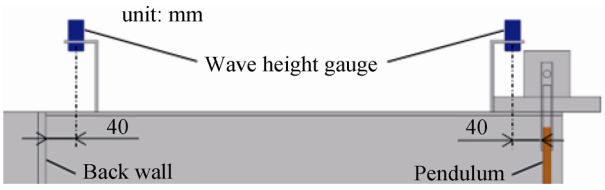

Fig. 2 Configuration of wave height gauges.

In this paper, the influence of distance between the back wall and the pendulum is investigated by shifting the pendulum from P = 0.650 m to 0.490 m and 0.325 m as shown in Fig. 4.

Experimental Results of Model with Servo Motors

Primary conversion efficiency

Figure 5 shows the torque Q and the rotational speed N measured by the servo motors as shown in Fig. 1, where (a) of Motor a and (b) of Motor b denote the servo motors of the both ends of the pendulum shaft. In this experiment, the torque Q was controlled every 1 msec. so as to keep the damping coefficient C_P (= Q/ω : Nm·s/rad., Q: torque, ω: angular speed) constant. The incident wave energy E_{in}, the output energy E_{out} and the primary conversion efficiency η_1 are obtained by the following equations:

$$E_{in} = \frac{\pi}{2kT} B \left(\frac{H}{2}\right)^2 \rho g \left(1 + \frac{2kh}{\sinh 2kh}\right) \quad (1)$$

$$E_{out} = \frac{1}{T}\int_0^T P_{out}(t)dt \quad (2)$$

$$\eta_1 = E_{out} / E_{in} \quad (3)$$

where H is the incident wave height, T is the wave period, k is the wave number, ρ is the density of water, g is the

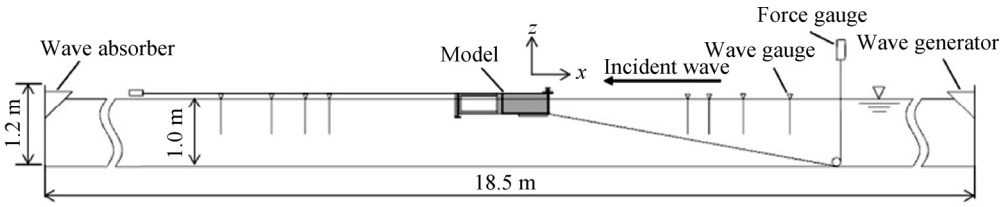

Fig. 3 Experimental equipment configuration in wave tank.

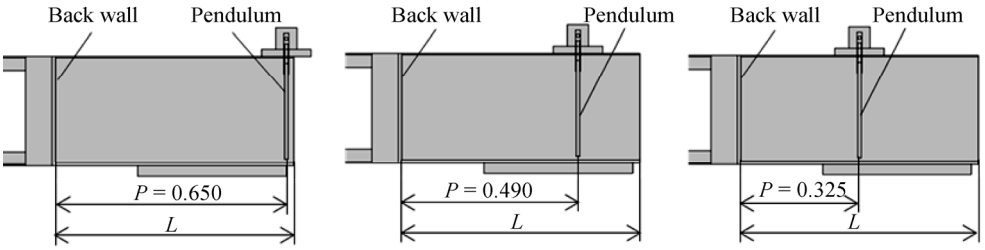

Fig. 4 Location of pendulum.

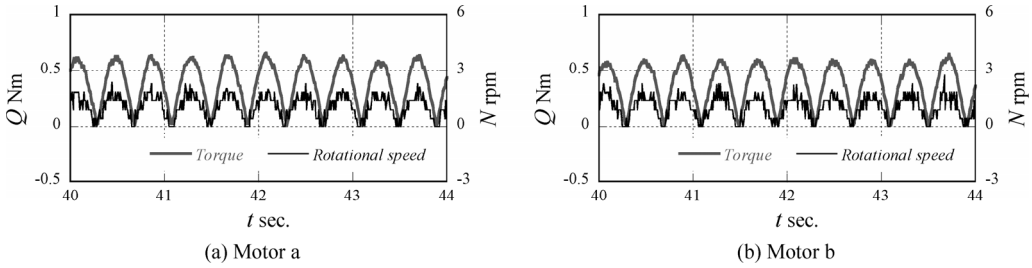

Fig. 5 Torque and rotational speed of pendulum shaft.

gravitational acceleration, h is the water depth, B is the width of the FPWEC, and P_{out} (= $Q\omega$) is the output.

Figures 6 and 7 show the primary conversion efficiencies, where Fig. 6 is the variations due to the incident wave length λ and Fig. 7 is the variations of the damping coefficient C_P. In these figures, the wave length λ was normalized by the chamber length L, and (a), (b) and (c) show the cases of P = 0.650 m, 0.490 m and 0.325 m respectively. Regardless of the pendulum position and the wave length, the primary conversion efficiency increases according to the increase of C_P from 1.8 to 5.2 Nm·s/rad. as shown in Fig. 7. In the case of P = 0.650 m, the maximum efficiency of 0.98 was achieved at C_P = 6.0 Nm·s/rad. and λ/L = 1.5. On the other hand, the high efficiencies of 0.91 and 0.90 were obtained at C_P = 5.2 Nm·s/rad. in the cases of P = 0.490 m and 0.325 m respectively. The above high efficiency is caused by coincidence of the pendulum position and the node position of the standing wave in the water chamber.

Wave height in water chamber

Figure 8 shows the wave displacement at the water chamber, where ζ_i denotes the incident wave amplitude, ζ_1 denotes the water level at 40 mm lee side from the pendulum plate and ζ_2 denotes the water level at 40 mm weather side from the back wall. In the case of P = 0.650 m at λ/L = 1.5, the amplitude of ζ_1/ζ_i is smaller than the case of λ/L = 2.0. This result of λ/L = 1.5 means that the pendulum position coincides with the node of the standing wave, namely the second mode having the wave length of 4/3 times that of P = 0.650 m as shown in Fig. 9(b). In contrast, the pendulum coincides with the antinode of the standing wave at λ/L = 2.0. Furthermore, the amplitude of ζ_1/ζ_i decreases remarkably at λ/L = 3.5. In the cases of P = 0.490 m and 0.325 m as shown in Figs. 8(b) and (c), the amplitude of ζ_1/ζ_i is small at λ/L = 3.0 and 2.5 respectively. These results of λ/L = 3.5, 3.0, 2.5 mean that the pendulum position coincides with the node of the standing wave, namely the first mode having the wave length of 4 times that of P as shown in Fig. 9(a). It is noticed that the λ/L of which the standing waves of the first and second modes occur becomes smaller as the pendulum position approaches the back wall as shown in Figs. 6 and 8.

Motions of floating body

Figure 10 shows the motion amplitude, where (a) shows the case of the first mode and (b) shows the

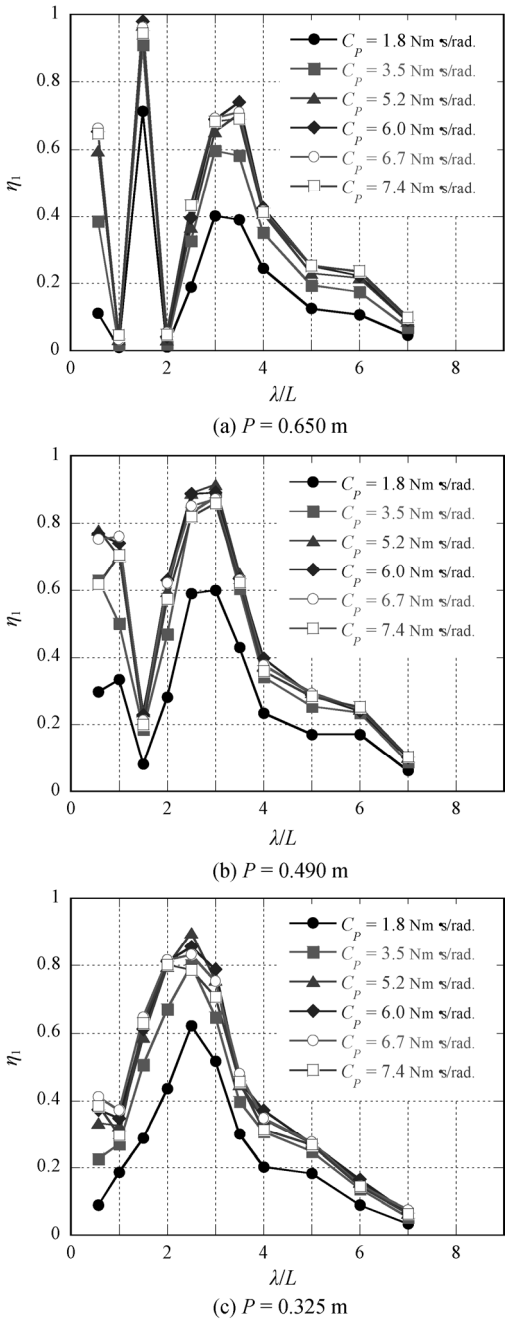

(a) P = 0.650 m

(b) P = 0.490 m

(c) P = 0.325 m

Fig. 6 Changes in primary conversion efficiency due to wave length.

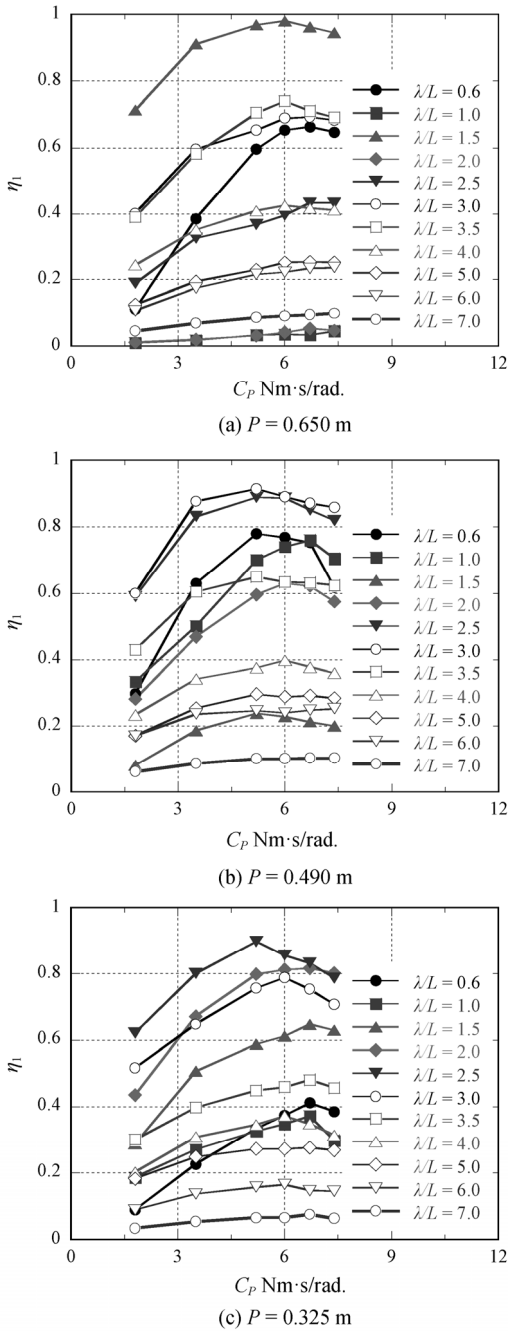

(a) P = 0.650 m

(b) P = 0.490 m

(c) P = 0.325 m

Fig. 7 Changes in primary conversion efficiency due to damping coefficient.

second mode. X/ζ_i, Z/ζ_i and $\Theta/k\zeta_i$ denote the surge amplitude, the heave amplitude and the pitch amplitude respectively. In Fig. 10(b) of the second mode, it is noticed that the motion of the floating body is significantly small.

In Fig. 10(a) of the first mode, the motion amplitude became larger than the case of the second mode regardless of the pendulum position. In all three cases of P = 0.650 m, 0.490 m and 0.325 m, the motion amplitude was reduced as C_P increase. Besides, the motion amplitude became smaller in the case of P = 0.325 m. This means that the vortex based on the motions is hardly generated around the floating body in the case of P = 0.325 m.

Power Generation Tests

Model with power take-off system

Although the secondary conversion system is unopti-

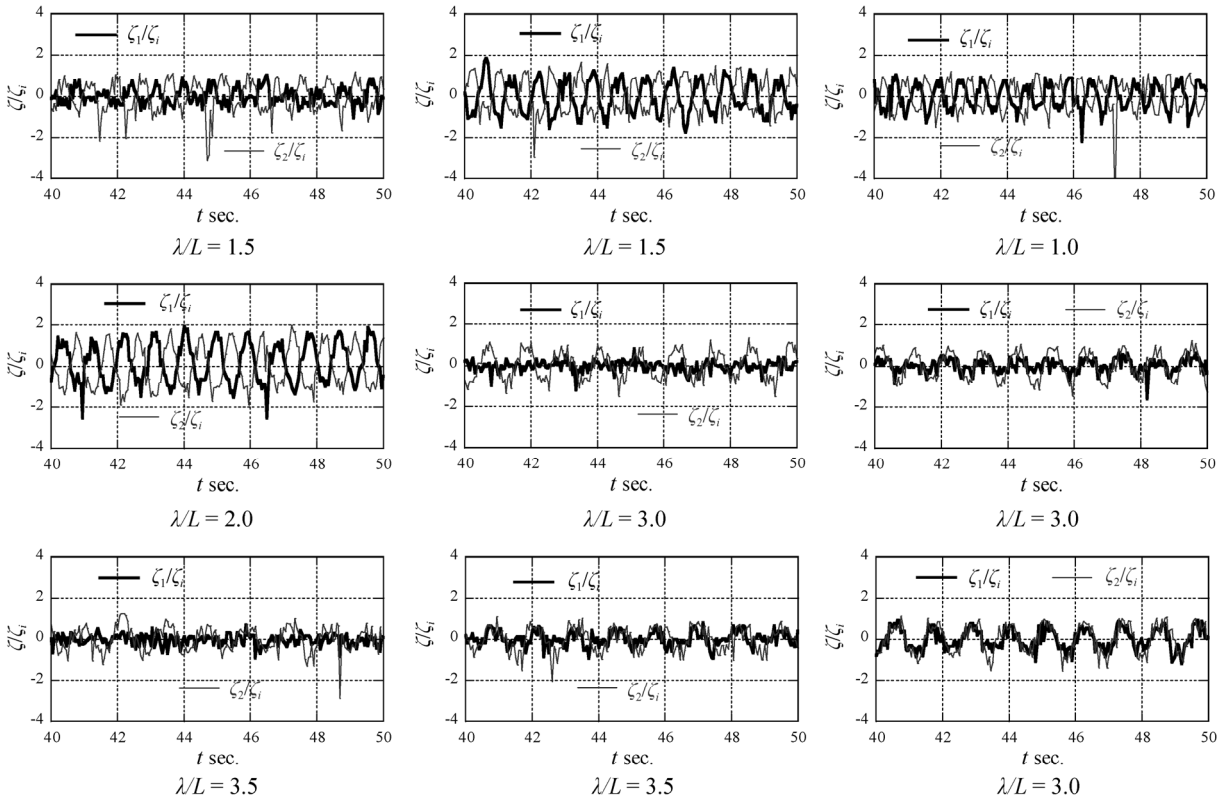

(a) P = 0.650 m, C_P = 6.0 Nm • s/rad. (b) P = 0.490 m, C_P = 5.2 Nm • s/rad. (c) P = 0.325 m, C_P = 5.2 Nm • s/rad.

Fig. 8 Water displacement in water chamber.

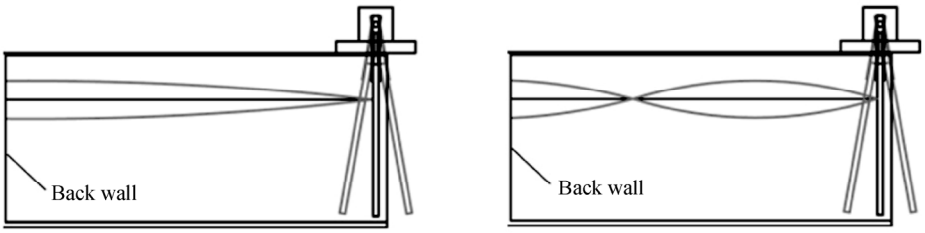

(a) First mode (b) Second mode

Fig. 9 Standing waves in water chamber.

mized, the generating efficiency was investigated by replacing the servomotors with the power take-off system composed of pulleys, belts and a generator. Figure 11 shows the power take-off system. The rotational speed of the pendulum shaft is multiplied by 28.8 by using the 6 pulleys and 3 belts. The output of the generator (SKY-denshi SKY-HR125) is 36 W at 600 r/min. To rectify the three phase alternating current, the AC-DC converter (Shindengen S10VTA60) was installed. The generating output was absorbed by a cement resistor. In this experiment, the cement resistor was varied from 50 Ω to 100 Ω, 200 Ω, 300 Ω and 400 Ω. The pendulum position is P = 0.650m giving the maximum primary conversion efficiency of η_1 = 0.98. The output P_{out} was calculated by the following equation:

$$P_{out} = V^2 / R \tag{4}$$

where V is the induced voltage and R is the resistor.

Generating efficiency

Figures 12 and 13 show the generating efficiencies, where Fig. 12 shows the variations due to the wave length λ/L and Fig. 13 shows the variations due to the resistor R. In Fig. 12, the peaks of the generating efficiency η appeared at almost the same λ/L as shown in Fig. 6(a) of the primary conversion efficiency, although the values are low. Besides, the maximum generating efficiency was achieved at R = 300 Ω as shown in Fig. 13.

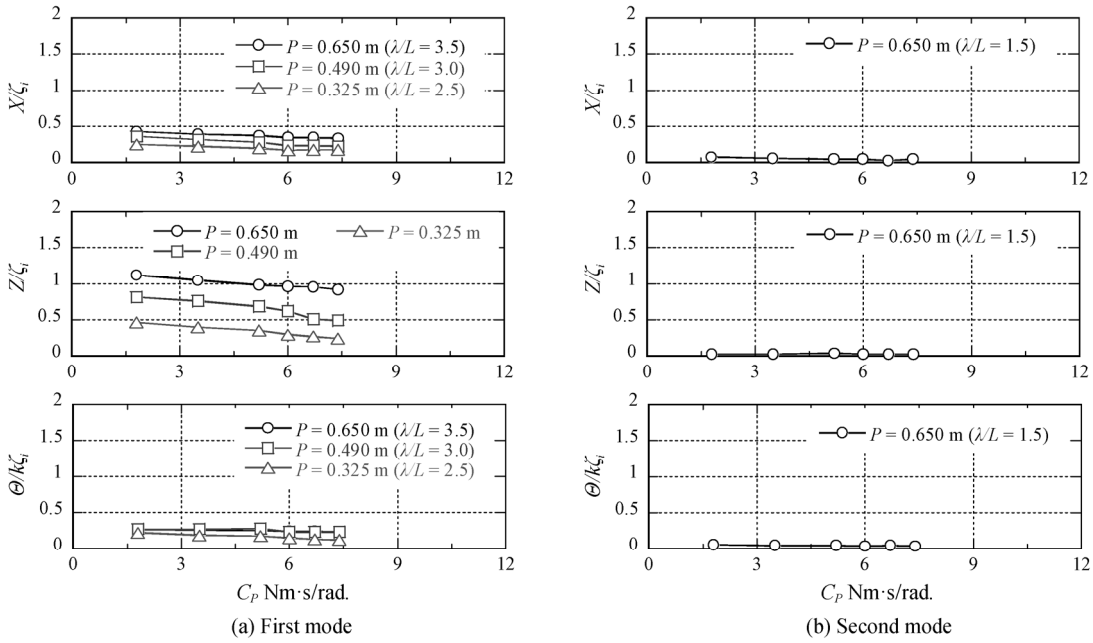

Fig. 10 Motion amplitude of floating body.

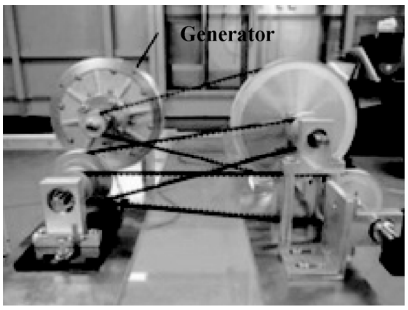

Fig. 11 Power take-off system.

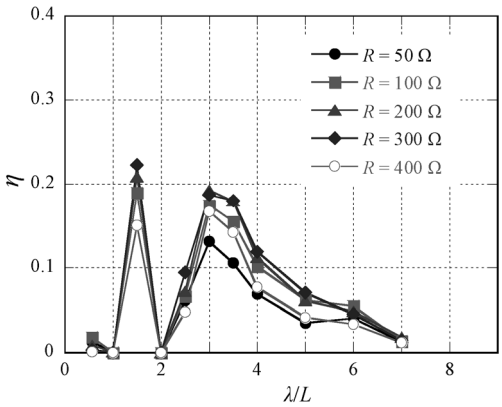

Fig. 12 Changes in generating efficiency due to wave length.

Motions of floating body and pendulum

The motions of the floating body are compared in Fig. 14 between the two cases giving the high efficiencies with the servo motors and with the generator, where the abscissa is the wave length λ/L. It is noticed that the motions of the floating body in the case with the generator are remarkably-similar to that of the case with the servo motors.

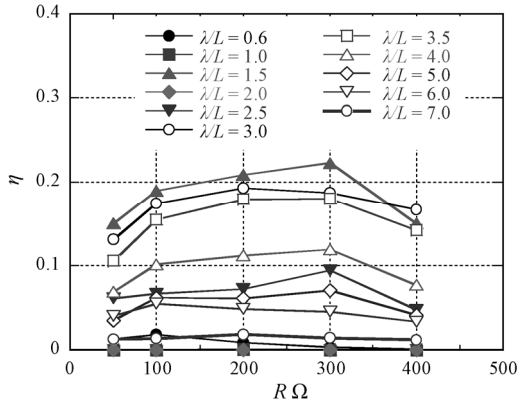

Fig. 13 Changes in generating efficiency due to electric resistor.

Figure 15 shows the rotational speed N of the pendulum shaft at the first and second modes, where (a) denotes the case with the servo motors and (b) denotes the case with the generator. The rotational speed of the pendulum shaft was averaged over a range of one wave period. The rotational speed became lower according to the increase of the resistor R and the damping coefficient C_P. In addition, it was clarified that the high primary conversion efficiency obtained at C_P = 6.0 Nm·s/rad. and the high generating efficiency obtained at R = 300 Ω are achieved at about N = 1.2 r/min. The authors will refine

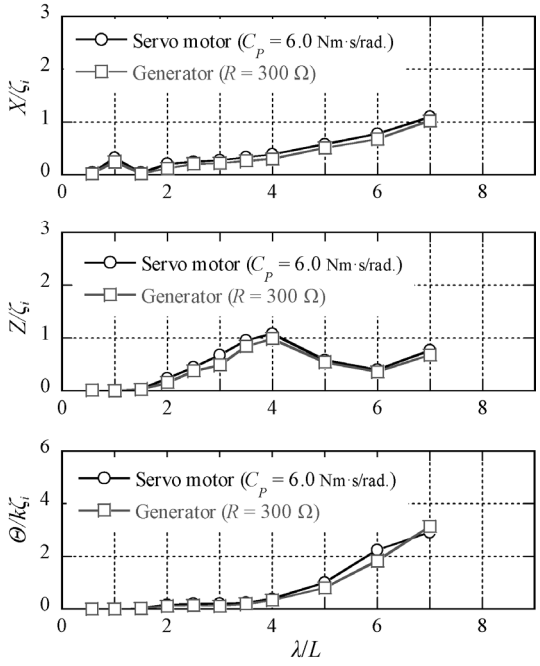

Fig. 14 Comparison between servo motor and generator on motion amplitude.

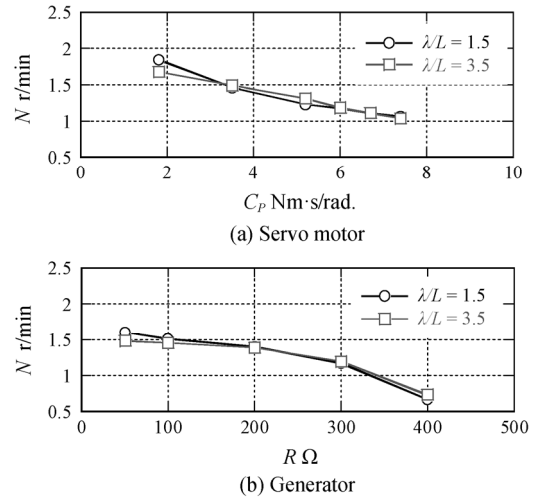

Fig. 15 Rotational speed of pendulum shaft in first and second modes.

the power take-off system so as to enable a highly efficient operation even though the rotational speed of the pendulum shaft is N = 1.2 r/min, and demonstrate the high performance in the field test in the near future.

Conclusions

This paper discussed the load characteristics of FPWEC and the motions of the floating body in regular wave. The following concluding remarks are obtained.

(1) The maximum primary conversion efficiency is achieved as high as 98% when the second mode occurs in the water chamber.

(2) Even in the first mode, the high primary conversion efficiency of 91% is obtained.

(3) In the first mode, the motion amplitude of the floating body was reduced as the damping coefficient increase.

(4) The high efficiency was achieved under the condition that the rotational speed of the pendulum shaft is about 1.2 r/min.

References

[1] Watabe, T.: Utilization of the Ocean Wave Energy, Fuji Print Press, (2008).

[2] Toyota, K., Nagata, S., Imai, Y., Ono, K. and Setoguchi, T.: Energy Conversion Characteristics on Floating Type Pendulum Wave Energy Converter in Regular Waves, Proceedings of the Twenty-first (2011) International Offshore and Polar Engineering Conference, Hawaii, USA, pp.675–679, (2011).

[3] Park, J. Y., Shin, S. H., Hong, K. Y. and Kim, S. H.: A Study on the Wave Response and Efficiency of a Pendulum Wave Energy Converter, Proceedings of the Twenty-second (2012) International Offshore and Polar Engineering Conference, Rhodes, Greece, pp.601–606, (2012).

[4] Nam, B. W., Hong, S. Y., Shin, S. H.: A Study on Wave-induced Motion of Floating Pendulum Wave Energy Converter, Proceedings of Asian Wave and Tidal Conference Series, Jeju, Korea, pp.124–128, (2012).